Czél, G., Jalalvand, M., & Wisnom, M. R. (2015). Demonstration of pseudo-ductility in unidirectional hybrid composites made of discontinuous carbon/epoxy and continuous glass/epoxy plies. Composites Part A: Applied Science and Manufacturing, 72, 75-84. 10.1016/j.compositesa.2015.01.019

Composites: Part A 72 (2015) 75–84

Contents lists available at ScienceDirect

Composites: Part A

journal homepage: www.elsevier.com/locate/compositesa

Demonstration of pseudo-ductility in unidirectional hybrid composites made of discontinuous carbon/epoxy and continuous glass/epoxy plies

Gergely Czél *, Meisam Jalalvand, Michael R. Wisnom

Advanced Composites Centre for Innovation and Science, University of Bristol, Queen's Building, Bristol BS8 1TR, United Kingdom

ARTICLE INFO

Article history:
Received 22 August 2014
Received in revised form 14 January 2015
Accepted 24 January 2015
Available online 2 February 2015

Keywords:
Discontinuous-ply composites
B. Delamination
C. Damage mechanics
D. Mechanical testing

ABSTRACT

A new, partially discontinuous architecture is proposed to improve the mechanical performance of pseudo-ductile, unidirectional (UD) interlayer carbon/glass hybrid composites. The concept was successfully demonstrated in different laminates with high strength and high modulus carbon and S-glass epoxy UD prepregs. The novel hybrid architecture provided pseudo-ductile tensile stress–strain responses with a linear initial part followed by a wide plateau and a second linear part, all connected by smooth transitions. The best hybrid configuration showed 60% improvement in modulus compared to pure glass, 860 MPa plateau stress and 2% pseudo-ductile strain. The initial modulus, the plateau stress and the overall tensile stress–strain response of each specimen configuration were predicted accurately.

1. Introduction

High performance composites provide excellent specific strength and stiffness properties especially in comparison with higher density metallic materials but fail to deliver a safe failure mode similar to metals' progressive yielding and strain hardening with detectable warning and a wide margin before final failure. The failure of fibre reinforced composites is usually sudden and catastrophic with insufficient warning and low residual load bearing capacity. This unfavourable failure character results in conservative structural design incorporating cautious limits preventing the full exploitation of the outstanding mechanical performance of a whole family of materials. On the other hand composites are not even considered for some applications where loading conditions are not fully predictable and catastrophic failure cannot be tolerated. High performance ductile or pseudo-ductile composites are therefore of exceptional interest and could significantly widen the scope of applications towards transportation and civil engineering fields.

One of the basic strategies to create pseudo-ductility is hybridisation which can improve the failure mode of conventional composites by making it gradual and more distributed. Early work on hybrid composites [1–5] reported their potential to obtain gradual failure over a range of strains by mixing different types of fibres either by intimately mingling them [6–8] or by creating a ply-by-ply hybrid structure [9–12]. The previously reported gradual failure in hybrid composites was usually observed in the form of a significant load drop at the low strain fibre failure in unidirectional (UD) interlayer hybrid composites, which is the baseline for improvement in this study. The most straightforward interply (or interlayer) hybridisation [5] was performed within this study because this method showed promising scope for pseudo-ductility [13] and it can be realised using existing prepreg materials which keeps specimen manufacturing simple. Strong potential for demonstrating pseudo-ductility while maintaining high performance in UD composites was shown earlier by the authors [13–15] using emerging thin ply prepregs to suppress delamination in interlayer hybrid configurations. The main focus of researchers investigating thin-ply composites was to explore the change in damage modes due to more dispersed lay-up designs [16–18]. Their main conclusion is that the onset of damage is delayed in thin-ply composites because premature matrix cracking and delaminations can be suppressed due to the low energy release rate of thin plies in static loading, but the final failure in general becomes more brittle. Thin-ply laminates also show less interlaminar but more fibre damage under impact [19]. The suppression of delaminations can be exploited in thin-ply UD interlayer hybrid composites [13] to make the pull-out of the broken low strain material stable. One issue with the thin ply hybrids presented in [13] is, that the resulting carbon/glass volume ratio is relatively low if the thickness limit of around 85 μm for that specific material combination is kept and standard thickness glass plies are used. In order to overcome this limitation, a UD partially discontinuous architecture with a discontinuous carbon and continuous glass layers is proposed here which will be called the discontinuous hybrid configuration in the rest of the paper. The

* Corresponding author. Tel.: +44 (0) 117 33 15311; fax: +44 (0) 117 95 45360.
E-mail address: G.Czel@bristol.ac.uk (G. Czél).

http://dx.doi.org/10.1016/j.compositesa.2015.01.019
1359-835X/

discontinuous architecture of the carbon layer results in macroscopic (10–20 mm long) carbon/epoxy elements in the test specimens which will be referred to as carbon/epoxy platelets.

Numerous researchers studied discontinuous composites usually made of modified UD prepregs for various purposes. Cui et al. [20] studied the mode II fracture toughness of composite ply interfaces using UD glass/epoxy specimens with cut central plies. Wisnom and Jones [21] also used cut ply specimens under four point bending to study the delamination process both in tension and compression. Czél et al. [22] reported highly non-linear stress–strain curves for discontinuous overlapped UD carbon prepreg specimens, showing potential for pseudo-ductility. The effect of overlap zone geometry on the failure mode was analysed in detail. Matthams and Clyne [23,24] modified their prepreg plies with laser drilled holes to improve the formability of their UD carbon/PEEK and carbon/PPS thermoplastic matrix composites. Taketa et al. [25] also improved the formability of continuous prepregs by slitting them into unidirectionally arrayed chopped strands (UACS). Better cured composite properties were achieved than with the traditional SMC (sheet moulding compound) hot pressing technology, exploiting the perfect initial alignment of fibres in the UACS. Li et al. [26] developed the same concept further by introducing new slit patterns to improve the strength, material symmetry and flowability of UACS.

The scope of previous studies on discontinuous prepregs was either interlaminar damage and failure characterisation or improvement of the flow-or formability of continuous UD prepregs. The discontinuous prepreg layers in the experimental part of this study are integral elements of a hybrid laminate architecture carefully designed to exhibit controlled interlaminar damage initiation and stable mode II crack propagation which results in the stable pull-out of the carbon/epoxy platelets.

The key challenge of this study is to improve the tensile performance and extend the design envelope of previously developed UD pseudo-ductile thin-ply continuous carbon/glass interlayer hybrid composites [13] by increasing the carbon/glass ratio and the initial modulus of the hybrid laminates. Emphasis was also put on accurate prediction of the stress–strain response of the novel hybrid material architecture.

2. Specimen design and analysis

The basic concept of this work was inspired by the authors' recently published study on thin-ply hybrid pseudo-ductile composites [13], where some of the specimen configurations failed in an unfavourable way, developing unstable delaminations straight after the first crack in the low strain material of the interlayer hybrid plates. The unstable delamination resulted in a significant stress drop at the strain to failure of the low strain constituent and compromised the pseudo-ductility of the UD hybrid material in tension as shown in Fig. 1. The new specimen design is based on the novel idea of introducing periodic discontinuities (i.e. ply cuts perpendicular to the fibre direction) in the low strain layer of UD interlayer hybrid composites. The special partially discontinuous architecture based on organised carbon/epoxy platelets in continuous glass/epoxy composite layers allows for controlled interfacial damage initiation before any possible platelet fracture, therefore providing smooth transitions and a plateau between the linear parts of the stress–strain graph as shown on Fig. 1. Any sudden stress drop due to unstable delaminations can be prevented with this new architecture until the initiation of high strain material failure.

2.1. Specimen geometry

The specimens tested within the experimental part of the study were UD, parallel edge tensile specimens with glass/epoxy tabs

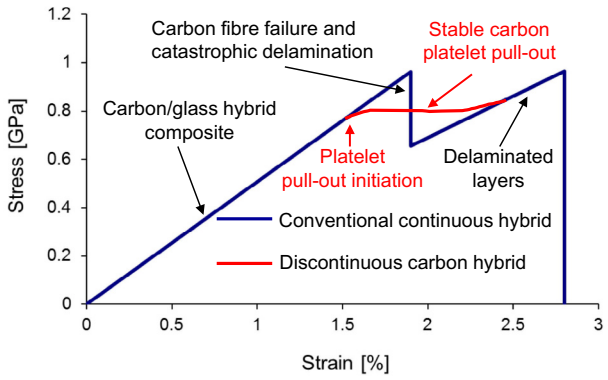

Fig. 1. Schematic of the expected stress–strain response of continuous carbon/continuous glass and discontinuous carbon/continuous glass UD hybrid laminates. (For interpretation of the references to colour in this figure legend, the reader is referred to the web version of this article.)

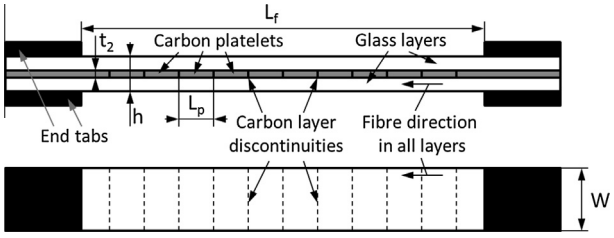

Fig. 2. Schematic of a UD discontinuous interlayer hybrid specimen.

bonded to the ends. Nominal specimen dimensions were 260/160/20/*h* mm overall length/L_f-free length/*W*-width/*h*-variable thickness respectively. Another important geometric parameter is the length of the discontinuous carbon/epoxy composite elements in the specimens which will be referred to as L_p-platelet length. Fig. 2 shows the geometric parameters on the side and top view schematics of a tensile specimen.

2.2. Materials

The materials considered for design, and used for the experiments were E-glass/913 and S-glass/913 epoxy prepregs supplied by Hexcel, and Sky Flex USN 020A and Sky Flex UPN 069A carbon/epoxy prepregs from SK Chemicals made with high strength Pyrofil TR30 and high modulus Pyrofil HS40 carbon fibres respectively, both produced by Mitsubishi Rayon. Both resin systems in the hybrid laminates were 120 °C cure epoxies, which were found to be compatible, although no details were provided by the suppliers on the chemical formulation of the resins. Good integrity of the hybrid laminates was confirmed during testing procedures and no phase separation was observed on cross sectional micrographs. Material data of the three prepreg systems can be found in Tables 1 and 2.

The G_{IIc} fracture toughness of the interfaces in various thickness TR30 carbon/epoxy and E-glass/epoxy hybrid laminates were studied earlier in [30] using specimens with a single cut in the carbon layer. A short summary of the key results is given in Table 3 and will be used for determination of the carbon/epoxy platelet pull-out stress in this study.

2.3. Ductility mechanism in tension

The new partially discontinuous architecture comprising carbon/epoxy platelets in continuous glass layers releases the previously established carbon layer thickness limitations [13] to

Table 1
Fibre properties of the applied UD prepregs (based on manufacturer's data).

Fibre type	Manufacturer	Elastic modulus (GPa)	Strain to failure (%)	Tensile strength (GPa)	Density (g/cm^3)
Pyrofil TR30 carbon	Mitsubishi Rayon	234	1.9	4.4	1.79
Pyrofil HS40 carbon	Mitsubishi Rayon	455	1.0	4.6	1.85
EC9 756 P109 E-glass	Owens Corning	72	4.5	3.5	2.56
FliteStrand S ZT S-glass	Owens Corning	88	5.5	4.8–5.1	2.45

Table 2
Cured ply properties of the applied UD prepregs.

Prepreg material	Property Unit	Fibre mass per unit area (g/m^2)	Cured ply thickness (mm)	Fibre volume fraction (%)	Initial elastic modulus (GPa)	Strain to failure (%)	Interlaminar shear strength (MPa)
TR30 carbon/epoxy	Average	21.2 [13]	0.029 [13]	41 [13]	101.7 [27]	1.9 [13]	–
	CoV[a] [%]	4.0 [13]	–	–	2.75 [27]	6.76 [13]	–
HS40 carbon/epoxy	Average	65[b]	0.070[b]	50[b]	229[b]	1.0[b]/1.15[d]	–
	CoV [%]	–	–	–	–	–	–
E-glass/epoxy	Average	192[b]	0.140 [13]	54 [13]	40[b]	3.7 [28]/2.8 [13][c]	100 [29]
	CoV [%]	–	–	–	–	–	–
S-glass/epoxy	Average	190[b]	0.155	50[b]	45.7	3.98	–
	CoV [%]	–	–	–	3	1.1	–

[a] Coefficient of variation.
[b] Based on manufacturer's data.
[c] Measured on different specimen types in tension.
[d] Measured in the continuous baseline specimens (see Table 4).

Table 3
Results of mode II fracture tests (designation: EG- E-glass, TR30- high strength carbon, with numbers corresponding to the number of plies of the constituent prepregs) [30].

Lay-up sequence	Property Unit	Modulus (GPa)	Delamination initiation strain (%)	G_{IIc} (N/mm)
2EG/4TR30/2EG	Average	53.1	1.60	1.10
	CoV [%]	2.4	–	–
4EG/8TR30/4EG	Average	50.2	1.26	1.35
	CoV [%]	1.6	1.4	–

assure progressive fragmentation and stable pull-out of the carbon layers in continuous carbon/glass hybrid configurations. The mode II energy release rate at the carbon layer failure strain should always be lower than the fracture toughness (G_{IIc}) in a continuous carbon/glass hybrid composite to avoid sudden delamination and load drops. But this criterion no longer has to be fulfilled in the discontinuous configurations, because stable delamination can initiate before carbon fibre failure. The discontinuities introduced in the carbon layer before curing the hybrid laminate can trigger the stable pull-out of the carbon/epoxy platelets at lower strains than the strain to failure of the carbon fibres, when the energy release rate becomes equal to the mode II fracture toughness of the glass-carbon composite interface. The stress level for carbon/epoxy platelet pull-out can be controlled by the thickness of the platelets and the continuous glass layers which together change the mode II energy release rate. However variable carbon/epoxy platelet thickness will result in different hybrid moduli due to the change in carbon/glass ratio and attention must be paid to ensure the continuous glass layers have enough strength to take the load shed by the pulled-out platelets.

2.4. Prediction of the initial tensile modulus of the discontinuous hybrids

The carbon/epoxy platelets contribute to the tensile stiffness of the hybrid laminate in a less favourable way than a continuous layer because of the presence of ineffective segments around the ends of each platelet. In order to optimise the platelet length of the hybrid laminates, the L_{pc} critical or ineffective length of the carbon/epoxy platelets (where the platelet is not fully loaded) has to be calculated using a similar formulation (1) to the one used on the fibre-matrix level to determine the critical fibre length, assuming a constant shear stress τ_{max} at the layer interface along the platelet.

$$L_{pc} = \frac{E_c \cdot \varepsilon_{c\,max} \cdot t_c}{\tau_{max}} \tag{1}$$

where E_c is the modulus of the carbon/epoxy platelets in the interlayer hybrid, $\varepsilon_{c\,max}$ is the strain to failure of the carbon fibres, t_c is the thickness of the carbon/epoxy platelets and τ_{max} is the interfacial shear strength of the glass–carbon composite interface. The matrix dominated interlaminar shear strength of the glass–carbon composite interface was assumed to be equal to the shear strength of the E-glass/epoxy composite for both glass prepregs (see Table 2).

There is a practical demand for low platelet length, because too long discontinuous segments may cause variability in the interaction with the features of the components made of the new type material. On the other hand the longer the carbon/epoxy platelets in the hybrid composite, the higher the contribution of the stiff carbon composite to the hybrid modulus, and the better the overall mechanical performance is. During the present study the platelet length was always kept higher than five times the ineffective length to retain high performance but keep the length scale of discontinuous elements in the hybrid architecture relatively low.

In order to assess the effect of discontinuities in the hybrid composite, let's assume the same force F applied on two different interlayer hybrid laminate configurations comprising a discontinuous and a continuous carbon layer of the same t_c thickness as shown in Fig. 3. Keeping the thickness of the glass layers consistent and assuming unit width, it is possible to connect the variable strains in the continuous glass plies through Eqs. (2), (3) written for different cross-sections (sections A and B in Fig. 3) at the middle and at the end of a carbon/epoxy platelet. An important condition

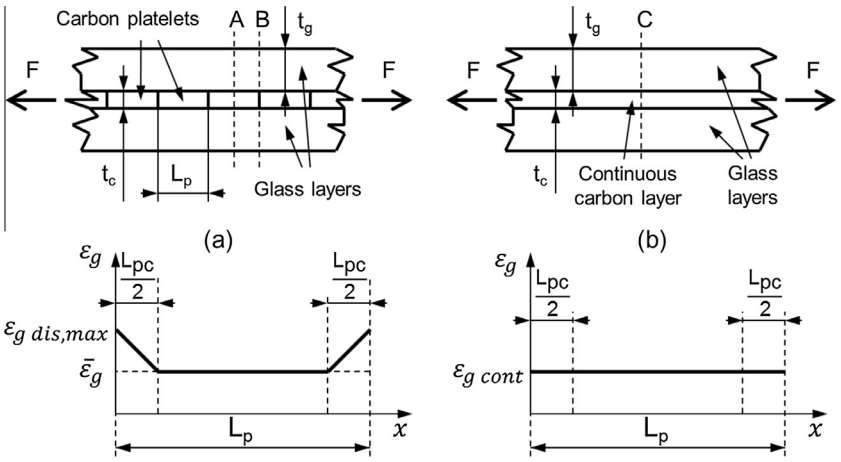

Fig. 3. Side view schematics of (a) discontinuous and (b) continuous carbon layer hybrid configurations with graphs showing the distributions of tensile strains in the glass layers for both configurations.

assumed during the analysis is that the longitudinal strains in the parallel layers are uniform and equal except for the sections corresponding to the ineffective parts of the carbon/epoxy platelets, where the strain in the carbon is lower and that in the glass layer is higher than elsewhere as shown on the lower graphs of Fig. 3.

Force per unit width at section A:

$$F = \bar{\varepsilon}_g(2 \cdot E_g \cdot t_g + E_c \cdot t_c) \tag{2}$$

Section B:

$$F = 2 \cdot \varepsilon_{g\,dis,max} \cdot E_g \cdot t_g \tag{3}$$

Eq. (4) gives the force formula for the continuous carbon configuration at section C:

$$F = \varepsilon_{g\,cont}(2 \cdot E_g \cdot t_g + E_c \cdot t_c) \tag{4}$$

where $\bar{\varepsilon}_g$ is the strain, away from the ends of the platelets in the continuous glass layer in the discontinuous hybrid, E_g and E_c are the moduli of the continuous glass and carbon composite layers respectively, t_g and t_c are the thicknesses of the glass and carbon layers respectively, $\varepsilon_{g\,dis,max}$ is the maximum strain arising in the continuous glass layer due to the discontinuity in the carbon layer and $\varepsilon_{g\,cont}$ is the strain in the continuous glass layer of the continuous carbon layer type laminate.

Equating Eqs. (2) = (4) it is obvious that $\bar{\varepsilon}_g = \varepsilon_{g\,cont}$ and it will be referred to as $\bar{\varepsilon}$ in the rest of the manuscript. Using Eqs. (2) = (3) the maximum strain in the glass layer of the discontinuous laminate can be calculated.

$$\varepsilon_{dis,max} = \bar{\varepsilon}\left(1 + \frac{E_c \cdot t_c}{2 \cdot E_g \cdot t_g}\right) \tag{5}$$

In order to work out the $E_{h\,dis}$ effective modulus of the discontinuous hybrid laminate, the elongations of the continuous glass layers of L_p length in the discontinuous and continuous architectures $\Delta L_{p\,dis}$ and $\Delta L_{p\,cont}$ respectively have to be analysed as in Eqs. (6) and (7).

$$\Delta L_{p\,dis} = \int_0^{L_p} \varepsilon_g\,dx = L_p \cdot \bar{\varepsilon} + \frac{L_{pc}}{2}(\varepsilon_{g\,dis,max} - \bar{\varepsilon}) = \bar{\varepsilon}\left(L_p + \frac{L_{pc} \cdot E_c \cdot t_c}{4 \cdot E_g \cdot t_g}\right) \tag{6}$$

$$\Delta L_{p\,cont} = L_p \cdot \bar{\varepsilon} \tag{7}$$

The $\varepsilon_{g\,av}$ average strain in the continuous glass layer of the discontinuous hybrid can be calculated using equation (8).

$$\varepsilon_{g\,av} = \frac{\Delta L_{p\,dis}}{L_p} = \bar{\varepsilon}\left(1 + \frac{L_{pc} \cdot E_c \cdot t_c}{4 \cdot L_p \cdot E_g \cdot t_g}\right) \tag{8}$$

The ratio between the overall effective moduli of the discontinuous and the continuous carbon/glass hybrid laminates can be calculated through the ratios of elongations, as the geometry and the applied overall stress is the same for both configurations.

$$K_d = \frac{E_{h\,dis}}{E_{h\,cont}} = \frac{\Delta L_{p\,cont}}{L_{p\,dis}} = \frac{L_p \cdot \bar{\varepsilon}}{\bar{\varepsilon}\left(L_p + \frac{L_{pc} \cdot E_c \cdot t_c}{4 \cdot E_g \cdot t_g}\right)} = \frac{1}{1 + \frac{L_{pc} \cdot t_c \cdot E_c}{4 \cdot L_p \cdot t_g \cdot E_g}} \tag{9}$$

This ratio can be defined according to Eq. (9) as the Discontinuity Knock-down Factor K_d which can be applied to the elastic modulus of the continuous carbon/glass hybrid laminate $E_{h\,cont}$ formulated in [13] and given here in Eq. (10a) to get the hybrid modulus of the discontinuous laminate $E_{h\,dis}$ according to Eq. (10b).

$$E_{h\,cont} = \frac{E_c t_c + E_g t_g}{t_c + t_g} \tag{10a}$$

$$E_{h\,dis} = K_d \cdot E_{h\,cont} \tag{10b}$$

It is interesting to note, that the reduction in stiffness due to the discontinuities depends on two purely configuration related parameters according to Eq. (9) (i.e. the ineffective length to platelet length ratio and carbon/epoxy platelet to glass layer thickness ratio) and one purely constituent material related parameter (i.e. the carbon to glass composite modulus ratio). It is clear that the carbon/epoxy platelet length L_p has a large impact on the initial modulus of the hybrid laminate and has to be kept large enough not to knock down the stiffness contribution of the carbon/epoxy platelets too much.

2.5. Criteria for pseudo-ductility and prediction of platelet pull-out stress

(i) To assure pseudo-ductility, it is crucial to make sure the continuous glass layers can take the extra load at the initiation of carbon/epoxy platelet pull-out to avoid premature glass failure and allow for a stress plateau. A criterion (Eq. (11)) was given earlier in [13] for continuous carbon hybrid laminates at carbon layer fracture, based on the redistribution of stresses, ignoring stress concentrations. Although the discontinuous hybrids are designed to avoid platelet fracture, the formula can be used as an estimate of the lower bound

for glass layer strength because of the similar stress fields around a carbon layer fracture in a continuous carbon hybrid and close to the end of a platelet in a discontinuous hybrid.

$$S_{g\,min} = \frac{S_c(E_g \cdot t_g + E_c \cdot t_c)}{E_c \cdot t_g} \tag{11}$$

where $S_{g\,min}$ is the minimum required strength of the glass composite and S_c is the strength of the carbon/epoxy platelets.

(ii) In order to make the new discontinuous material architecture pseudo-ductile, any sudden stress drop in the stress–strain response of a monotonic displacement controlled tensile test has to be avoided. To fulfil this need, the configuration has to be designed to avoid any platelet fracture and to allow stable platelet pull-out. It is therefore necessary to design the architecture to release enough energy to initiate stable delamination of the carbon/epoxy platelets at a lower overall stress than that corresponding to their fracture. This requirement can be formulated as in Eq. (12) to keep the $G_{II\,carb.fract.}$ energy release rate at carbon fracture higher than the G_{IIc} mode II fracture toughness of the interface.

$$G_{II\,carb.fract.} > G_{IIc} \tag{12}$$

Eqs. (13a) and (13b) can be used to determine the mode II energy release rate of a continuous carbon layer embedded in glass layers. The following assumptions were made when Eqs. (13a) and (13b) were formulated earlier in [13]: the strain before delamination within the volume of the hybrid laminate as well as the average stress during delamination are constant.

$$G_{II} = \frac{\varepsilon^2 E_c t_c (E_g(h - t_c) + E_c t_c)}{4E_g(h - t_c)} \tag{13a}$$

$$G_{II} = \frac{\sigma^2 h^2 E_c t_c}{8E_g t_g (2E_g t_g + E_c t_c)} \tag{13b}$$

where ε is the remote tensile strain in the laminate, h is the full thickness of the laminate and σ is the overall average tensile stress in the laminate. These formulations can also be applied to the discontinuous configurations for design purposes provided that the platelets are long enough compared to the ineffective platelet length, which is the case here. Eq. (13a) is suitable to estimate the $G_{II\,carb.fract.}$ energy release rate at carbon fracture if the carbon failure strain is substituted. If Eq. (13b) is reordered, and the fracture toughness of the glass–carbon interface is substituted, the interlaminar crack propagation stress can be estimated with equation (14), which corresponds to the plateau in the stress–strain graph due to stable pull-out of the carbon/epoxy platelets from the continuous glass/epoxy layers.

$$\sigma_{pull\text{-}out} = \sqrt{\frac{8G_{IIc}E_g t_g (2E_g t_g + E_c t_c)}{h^2 E_c t_c}} \tag{14}$$

2.6. Prediction of the tensile behaviour

A basic approach was applied here to predict the tensile stress–strain response of UD discontinuous hybrid laminates. The first part of the curve was estimated with a straight line of $E_{h\,dis} = K_d \cdot E_{h\,cont}$ slope starting from the modulus of a continuous carbon layer hybrid and applying the Discontinuity Knock-down Factor from Eq. (9). This line is turned into a straight horizontal plateau at the platelet pull-out stress calculated with Eq. (14). The post pull-out part of the predicted stress–strain response is calculated on the basis of assuming no contribution to the stiffness from the fully pulled-out carbon/epoxy platelets. The slope of this part of the curve which is the $E_{h\,fin.}$ "final hybrid modulus" can be formulated with Eq. (15).

$$E_{h\,fin.} = \frac{E_1(h - t_c)}{h} \tag{15}$$

Although very limited residually bonded areas (less than 1 mm wide dark lines in Fig. 4) were expected and observed on each carbon/epoxy platelet, the contribution of these to the laminate stiffness was very low and therefore neglected. Fig. 4 shows a typical prediction curve along with images of a [2SG/4TR30/2SG]-13 mm type specimen (see Table 4 for specimen details) at different stages of the damage process.

3. Experimental

A detailed discussion of specimen types, manufacturing, test methods and tensile test results is given in this section.

3.1. Specimen types

Table 4 shows the specimen configurations tested. Some calculated values are also included in the table such as the K_d hybrid modulus Discontinuity Knock-down Factor and the energy release rate at carbon failure strain. Please note, that the fracture toughness values used for pull-out stress predictions were different for thinner and thicker specimen types based on experimental results reported in Table 3. The calculated energy release rates at the carbon/epoxy platelet strain to failure being higher than the fracture toughness of the corresponding specimen configurations indicate that the platelet pull-out will initiate before platelet failure.

The first four configurations with low carbon/glass ratios were designed to be safe against premature glass failure and to allow

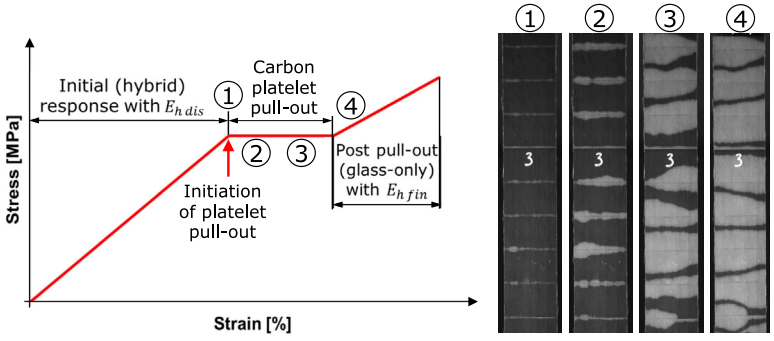

Fig. 4. Typical prediction of a discontinuous interlayer hybrid composite stress–strain response with images showing different stages of damage process in the specimens. (Dark areas show the bonded, while light areas show the delaminated parts of the hybrid specimen.) (For interpretation of the references to colour in this figure legend, the reader is referred to the web version of this article.)

Table 4
Tested specimen configurations (designation: SG- S-glass, TR30- high strength carbon, HS40- high modulus carbon, with numbers corresponding to the number of plies of the constituent prepregs).

Lay-up sequence	Platelet length L_p (mm)	Nominal thickness (mm)	Nominal carbon/ glass volume ratio (–)	Ineffective platelet length L_{pc} (mm)	Hybrid modulus Discontinuity Knock-down Factor K_d (–)	Calculated G_{II} at carbon strain to failure (N/mm)	Measured G_{IIc} for thickness (N/mm)
2SG/4TR30/2SG	Cont. baseline	0.736	0.153	–	–	1.43	1.10
2SG/4TR30/2SG	25	0.736	0.153	2.15	0.983	1.43	1.10
4SG/8TR30/4SG	25	1.472	0.153	4.30	0.967	2.86	1.35
2SG/4TR30/2SG	13	0.736	0.153	2.15	0.968	1.43	1.10
1SG/3TR30/1SG	Cont. baseline	0.397	0.229	–	–	1.23	1–1.1[a]
1SG/3TR30/1SG	10	0.397	0.229	1.61	0.970	1.23	1–1.1[a]
1SG/3TR30/1SG	10, only 1 ply cut	0.397	0.229	1.61	1[c]	1.23	1–1.1[a]
1SG/1HS40/1SG	Cont. baseline	0.380	0.227	–	–	1.14[b]	1–1.1[a]
1SG/1HS40/1SG	12	0.380	0.227	1.85	0.919	1.14[b]	1–1.1[a]

[a] Estimated range (1 N/mm is the extrapolation of measured data for lower specimen thicknesses).
[b] Using a measured strain to failure of $\varepsilon_{c\,max} = 1.15\%$ for HS 40 carbon/epoxy.
[c] Assuming a quasi-continuous carbon layer.

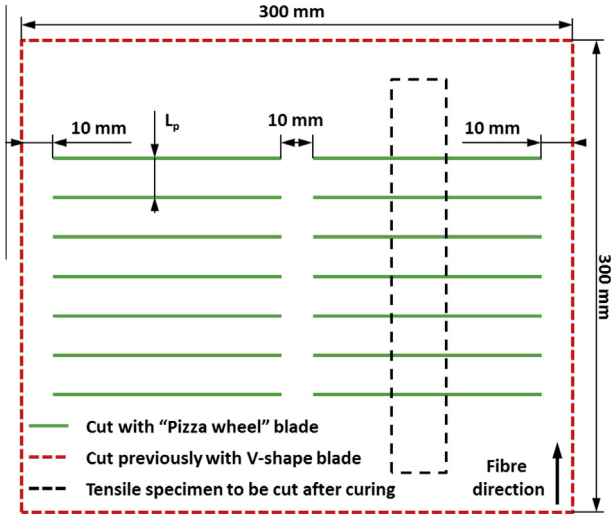

Fig. 5. Cut pattern for the carbon layers of the discontinuous hybrid composite plates showing a position where a typical specimen is cut out from. (For interpretation of the references to colour in this figure legend, the reader is referred to the web version of this article.)

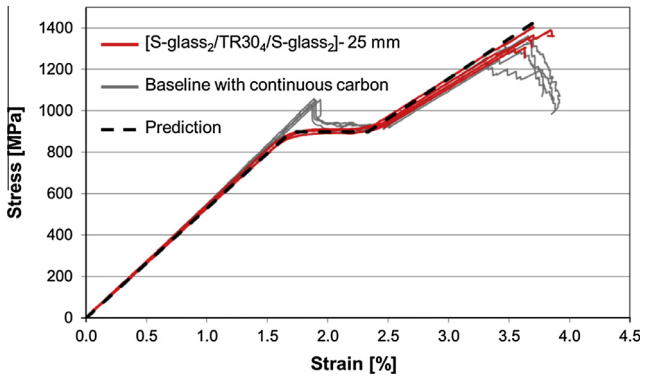

Fig. 6. Stress–strain curves of the [2SG/4TR30/2SG]-25 mm type specimens compared to those of the continuous baseline specimens. (For interpretation of the references to colour in this figure legend, the reader is referred to the web version of this article.)

for analysis of the effects of specimen thickness and platelet length. The rest of the specimens have higher carbon/glass ratios combined with shorter platelets and are designed for maximum performance. There is also a special version of the [1SG/3TR30/1SG]-10 mm configuration with only one of the three carbon plies cut to explore the possible benefits of pre-weakening the carbon plies. The key feature of this novel configuration is that the otherwise detrimental stress-concentrations can be exploited to form platelets from a partially discontinuous carbon layer in-situ under load. This way the initial stiffness of a continuous carbon/glass hybrid plate can be almost fully retained, but in the damage progression phase it behaves similarly to the fully discontinuous carbon layer configuration.

3.2. Specimen manufacturing

The new type composites involving discontinuous prepreg plies needed new manufacturing procedures, especially to make sure the performance of the fibres around the discontinuities in the prepreg is not affected by the cutting technique and that the cuts are aligned accurately during lay-up. A 25 mm diameter "pizza wheel" blade was found to be suitable to reduce the shearing of the uncured prepreg when fabricating the sensitive internal cuts (see Fig. 5). The less important circumferential cuts around the outside edges of the plies were made with a standard V-shape blade which cuts faster and is easier to set up, but introduces more shear deformation to the prepreg.

The steps of the manufacturing route for the cut blocked ply specimens were the following:

1. Cutting the carbon prepreg to the size of the panel to be manufactured on a CNC ply cutter with a V-shape blade (see Fig. 5).
2. Laying-up the thin carbon plies to make the central layer of the interlayer hybrid.
3. Creating the periodic internal cuts in the uncured carbon prepreg ply block with a 25 mm diameter "pizza wheel" blade on a CNC ply cutter leaving uncut sections in the middle and at the sides of the panel to retain the alignment of the cuts during the next layer assembly step (see Fig. 5).
4. Attaching the central carbon layer to the outer glass ones and consolidating under vacuum.
5. Bagging the composite plate up in the usual way using a 2 mm silicone sheet on top of the prepreg plies to provide uniform pressure distribution and good surface finish.

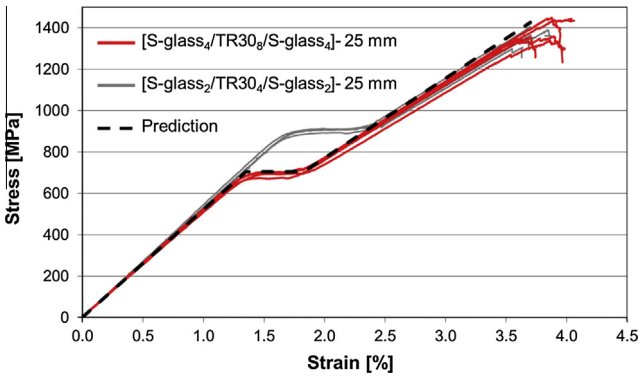

Fig. 7. Stress–strain curves of the scaled thickness [4SG/8TR30/4SG]-25 mm type specimens compared to those of the [2SG/4TR30/2SG]-25 mm type baseline specimens. (For interpretation of the references to colour in this figure legend, the reader is referred to the web version of this article.)

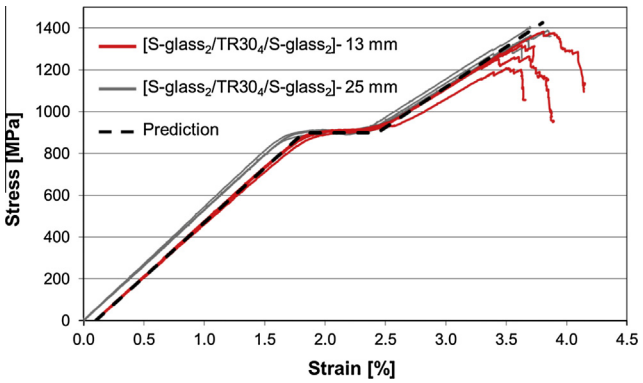

Fig. 8. Stress–strain curves of the [2SG/4TR30/2SG]-13 mm type specimens compared to those of the [2SG/4TR30/2SG]-25 mm type baseline specimens. (Curves of the shorter platelet specimens were offset from the origin by 0.1% strain for clearer comparison.) (For interpretation of the references to colour in this figure legend, the reader is referred to the web version of this article.)

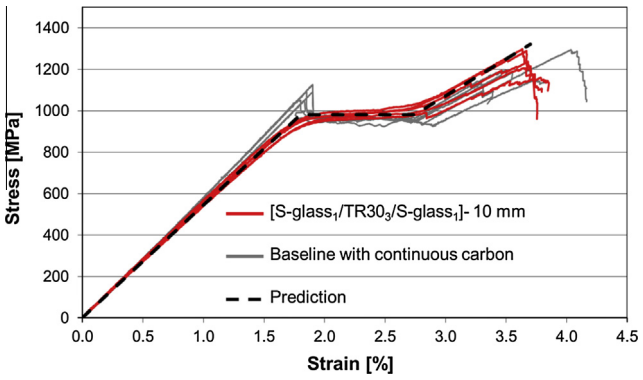

Fig. 9. Stress–strain curves of the [1SG/3TR30/1SG]-10 mm type specimens compared to those of the continuous baseline specimens. (For interpretation of the references to colour in this figure legend, the reader is referred to the web version of this article.)

6. Curing the composite plate in an autoclave using the recommended cure cycle (1 h@125 °C and 0.7 MPa).
7. Fabrication of individual specimens with a diamond cutting wheel.

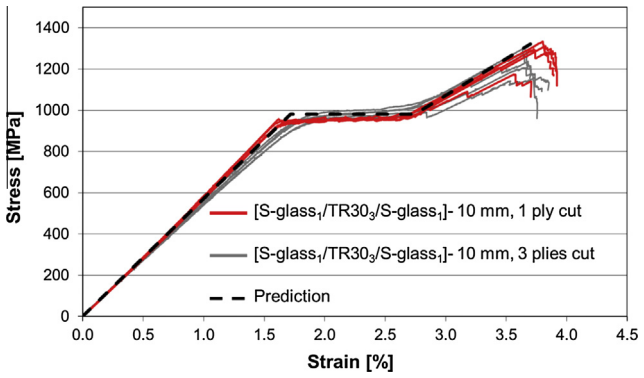

Fig. 10. Stress–strain curves of the [1SG/3TR30/1SG]-10 mm pre-weakened type specimens compared to those of the normal [1SG/3TR30/1SG]-10 mm type. (Please note that the prediction curve corresponds to the continuous carbon configuration). (For interpretation of the references to colour in this figure legend, the reader is referred to the web version of this article.)

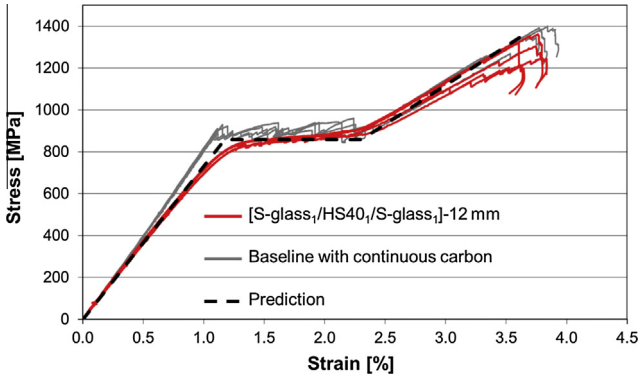

Fig. 11. Stress–strain curves of the [1SG/1HS40/1SG]-12 mm type specimens compared to those of the continuous baseline specimens. (For interpretation of the references to colour in this figure legend, the reader is referred to the web version of this article.)

3.3. Test method

Testing of the parallel edge specimens was executed under uniaxial tensile loading and displacement control using a cross-head speed of 2 mm/min on a computer controlled Instron 8801 type 100 kN rated universal hydraulic test machine with wedge type hydraulic grips. Strains were measured using an Imetrum videogauge system with a nominal gauge length of 130 mm. Minimum five specimens were tested from each configuration.

4. Results and discussion

The tensile test results of the specimen configurations are discussed here in detail. Fig. 6 shows the stress–strain graphs of the [2SG/4TR30/2SG]-25 mm type carbon/S-glass hybrid specimens made with 25 mm long carbon/epoxy platelets, along with those of the corresponding continuous carbon baseline specimens. The platelets in this configuration are expected to be long enough to give a good contribution to the specimen stiffness resulting in similar hybrid modulus to that of the baseline specimens. The figure shows that the discontinuous carbon layer architecture improved the tensile failure character of the delaminating continuous hybrid configuration by replacing the significant (~15%) stress drop due to excess strain energy in the carbon layer with a very smooth and gradual degradation of the tangent specimen stiffness which can be referred to as *pseudo-yielding*. The demonstrated very benign failure

Table 5
Results summary of the tested hybrid composite configurations (The moduli were evaluated according to the nominal thickness of each configuration. Measured values are averages with numbers in brackets indicating the coefficients of variations in percent. Ductility parameters were determined graphically on the stress-strain curves of each series (five specimens).)

Lay-up sequence	Platelet length L_p (mm)	Predicted modulus (GPa)	Measured modulus (GPa)	Modulus increase to pure glass (%)	Predicted platelet pull-out stress (MPa)	Measured platelet pull-out stress (MPa)	Pseudo-yield strain[a] (%)	Approx. final failure strain (%)	Pseudo-ductile strain[b] (%)
2SG/4TR30/2SG	Cont. baseline	53.83	54.39 (1.0)	19.2	–	–	–	3.6	–
2SG/4TR30/2SG	25	52.99	53.01 (2.1)	16.2	899	896	1.82	3.7	1.31
4SG/8TR30/4SG	25	52.11	52.02 (1.5)	14.0	704	689	1.42	3.8	1.32
2SG/4TR30/2SG	13	52.18	51.74 (2.8)	13.4	899	902	1.85	3.5	1.24
1SG/3TR30/1SG	Cont. baseline	57.04	56.76 (1.3)	24.4	–	–	–	3.6	–
1SG/3TR30/1SG	10	54.48	54.73 (1.7)	19.9	981	977	1.86	3.6	1.46
1SG/3TR30/1SG	10, only 1 ply cut	57.04	56.78 (1.2)	24.4	981	948	1.76	3.7	1.61
1SG/1HS40/1SG	Cont. baseline	79.59	78.60 (2.9)	72.3	–	–	–	3.7	–
1SG/1HS40/1SG	12	73.17	73.30 (1.8)	60.6	858	852	1.20	3.7	2.02

[a] *Pseudo-yield points* were defined as the intersection of the test curve with a straight line parallel to the initial slope of the stress–strain graph with an offset of 0.1% strain (similar to the offset yield point or proof stress in metals terminology).

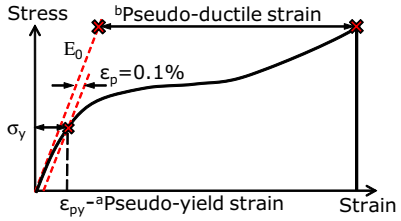

[b] *Pseudo-ductile strain* was defined between the strain of a point on the initial slope line at the *failure stress* (defined at the point where a 5% reduction in stress after the maximum has occurred) and the *strain at the failure stress*.

mode was achieved by making the carbon layer discontinuous and letting the carbon/epoxy platelets pull-out stably from the continuous glass layers. The platelet pull-out initiated earlier than the strain to failure of the carbon fibres as expected based on the calculated energy release rate in Table 4. Therefore platelet fractures and the corresponding load drops were avoided. The prediction based on the calculated initial hybrid modulus (Eq. (10b)), platelet pull-out stress (Eq. (14)) and final hybrid modulus (Eq. (15)) shows a very good correlation to the test data.

Fig. 7 shows the effect of specimen thickness on the failure process through tensile test results of two scaled thickness specimen types with the same carbon/epoxy platelet length. The primary difference between the responses of the specimen types is that in the thick case, the mode II energy release rate is higher so it exceeds the fracture toughness of the interface at a lower stress level and triggers the stable pull-out of the carbon/epoxy platelets earlier. The modulus and platelet pull-out stress prediction applying the fracture toughness measured for the higher thickness specimens was very accurate. A slight reduction in the initial stiffness due to scaling was also observed. This was expected because the platelet length was not scaled for practical reasons (only three 50 mm platelets would have fitted in the gauge length of the specimens).

Fig. 8 highlights the effect of the platelet length on the failure character of the interlayer hybrid configurations by plotting the tensile stress–strain curves of two specimen types with the same stacking sequence but various carbon/epoxy platelet lengths. Please note that the stress–strain plots of the shorter platelet specimens were offset from the origin by 0.1% strain for the sake of clearer comparison. The plots of Fig. 8 show only a small reduction in initial stiffness due to the decrease in the length of the carbon/epoxy platelets. This indicates that there may be scope for further reduction of the platelet length to make the new discontinuous material architecture more suitable for real components and structural applications.

Fig. 9 shows the stress–strain response of a more optimised specimen type together with the continuous baseline response. This specimen type has an increased carbon/glass ratio for high stiffness and the shortest platelet length for better applicability. [1SG/3TR30/1SG]-10 mm specimens show a very wide plateau because of the high carbon/glass ratio resulting in a high stiffness mismatch between the pure glass and the carbon reinforced hybrid layers. The plateau stress just below 1000 MPa is also respectable. The modulus increase due to hybridisation is 19.9% compared to the pure S-glass/epoxy composite and the failure type is changed completely by introducing pseudo-yielding.

Fig. 10 shows the response of a unique pre-weakened version of the [1SG/3TR30/1SG]-10 mm specimen type, where only the central one of the three carbon plies was made discontinuous. The periodic cuts in the central one of the three carbon plies produced stress concentrations high enough to fracture the continuous carbon plies at a stress level just below the platelet pull-out propagation stress, so any stress drops were avoided. This special architecture let the carbon-epoxy platelets form in-situ (by breaking-up of the partially cut carbon layer) and be pulled out stably from the continuous glass plies. The main reason for designing this configuration was to recover the initial modulus loss caused by cutting the carbon plies completely. The modulus of this specimen type was successfully restored to the same value (within experimental scatter) as that of the continuous baseline specimen configuration and provided up to 24.4% increase compared to that of the pure glass composite. The cracking of the continuous carbon plies started at slightly lower stresses than the plateau stress of the fully discontinuous type specimens of the same lay-up. The nature of the transition between the linear and the plateau part of the

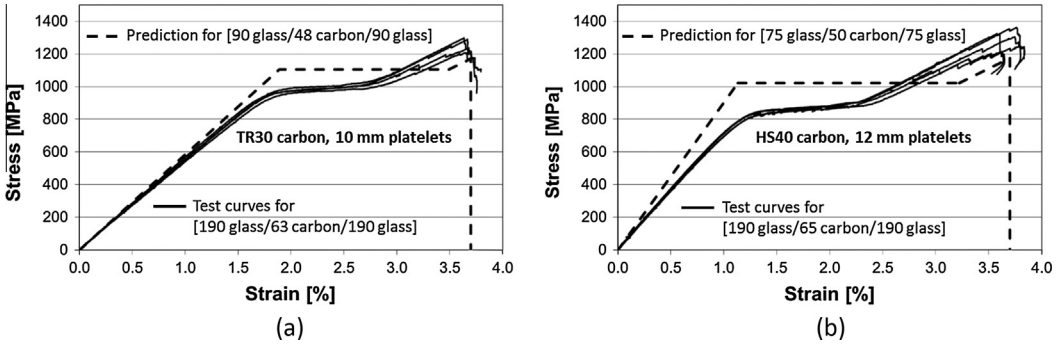

Fig. 12. Predictions for optimum setups hybridizing S-glass with (a) high strength TR30 carbon and (b) high modulus HS40 carbon, with fixed platelet lengths. The best available tested configurations are included as well for reference. (The numbers in the lay-up sequences indicate the mass per unit area of the fibres in the layers in [g/m^2]).

stress–strain curve has become less smooth compared to the corresponding fully discontinuous carbon layer specimen type. The reason for this, is that in the case of the fully discontinuous carbon/epoxy platelets the shear strain around the ends of the platelets is higher than elsewhere due to extra longitudinal strain in the glass (see Fig. 3) and lower longitudinal strain in the carbon. The shear stress concentrations around the ends of the platelets can lead to benign interlaminar damage initiation under monotonic loading and hence the stiffness is reduced in a very gradual way resulting in a smooth transition. On the other hand in the case of the pre-weakened carbon layer the platelets are formed in situ by fractures of the continuous carbon/epoxy plies which resulted in a more sudden change in the slope of the stress–strain curve.

Fig. 11 demonstrates the discontinuous hybrid composite ductility concept using a high modulus carbon fibre reinforced epoxy prepreg different from the high strength carbon prepreg used for the rest of the hybrid configurations. The results of the [1SG/1HS40/1SG]-12 mm configuration show that the concept also works well with this different material combination since the design criteria are met. The continuous [1SG/1HS40/1SG] baseline configuration shows an intermediate response between stable and unstable carbon layer pull-out after fragmentation. This is in agreement with the expectations based on the calculated mode II energy release rate of this configuration at the carbon failure strain, which is slightly above the fracture toughness of the interface (see Table 4). The load drops in the plateau strain regime of the continuous [1SG/1HS40/1SG] type specimens correspond to unstable delaminations occurring immediately after the fractures of the carbon layer. Normally in delaminating configurations there is only one single fracture across the carbon layer followed by immediate delamination to an extent depending on the excess energy released at the fracture of the carbon layer. This instant delamination then progresses stably towards the end tabs. The continuous [1SG/1HS40/1SG] specimens showed multiple fractures with small instantaneous delaminations each of which correspond to a stress drop in the stress–strain graph suggesting that the energy release rate was not significantly higher than the interlaminar fracture toughness to let the interlaminar cracks propagate far. Small variability in the interlaminar properties may have stopped the cracks propagating and let the carbon layer fracture again somewhere else. The failure type was changed completely by the introduction of the discontinuous carbon layer architecture in [1SG/1HS40/1SG]-12 mm specimens which allowed the interfacial damage to initiate and cracks propagate stably before any carbon/epoxy platelet fracture. Later, during the pull-out phase, some of the platelets fractured. This was not unexpected as the plateau stress of the discontinuous hybrid was very close to that of the continuous carbon layer type baseline. The energy release rate of this configuration was also just above the estimated fracture toughness of the interface, so even small variations in material properties could lead to a change in the damage process. It is interesting to note the just visible load drops in some of the red stress–strain curves of Fig. 11 which correspond to platelet fractures. The initial modulus and plateau stress of the [1SG/1HS40/1SG]-12 mm type hybrid specimens were predicted accurately. This configuration showed high initial modulus and a long pseudo-ductile plateau as well as a respectable pseudo-yield stress.

Table 5 summarises the results of all the tested discontinuous and continuous carbon type hybrid configurations. The agreement between the predicted and measured initial moduli and platelet pull-out stresses is good in general. The highest error of 3.5% was observed for the pull-out/plateau stress of the special pre-weakened [1SG/3TR30/1SG]-10 mm configuration, probably due to variability of the interfacial properties. The moduli of the discontinuous hybrid composites were increased significantly (13–60%) with respect to that of the pure glass/epoxy composites, although the pseudo-ductility was gained at the cost of a reduction in modulus and strength compared to the pure carbon/epoxy.

4.1. Scope for further optimisation

Although the higher carbon/glass ratio hybrids were close to optimal configurations there were serious limitations in terms of available materials. If these limitations are released, even better configurations can be designed as shown in Fig. 12. In general, the optimum configurations have thinner glass layers, initiate platelet pull-out very close to the strain to failure of the carbon/epoxy platelets, have high and wide plateaus, and limited stress margin between the plateau and the final failure stress.

5. Conclusions

The following conclusions were drawn from the extensive study of unidirectional discontinuous carbon/continuous glass fibre reinforced epoxy interlayer hybrid composites:

- Stable, progressive pseudo-ductile failure in tension with significant warning and margin before final failure was demonstrated with two different material combinations utilising the novel discontinuous hybrid architecture. Favourable stress–strain responses, with smooth transitions between the elastic and plateau strain regimes were achieved.
- The new discontinuous hybrid architecture made it possible to release the carbon layer thickness restrictions for pseudo-ductile tensile response in UD carbon/glass hybrid laminates allowing for an increased carbon/glass ratio and therefore higher initial hybrid modulus and plateau stress.

- The most optimised high modulus discontinuous carbon/epoxy configuration showed 60% modulus improvement to the baseline glass/epoxy composite along with a respectable 858 MPa stress plateau and 2% pseudo-ductile strain.
- The advanced pre-weakened high strength carbon layer architecture with only one of the three plies of carbon being discontinuous showed 24% modulus increase compared with the pure glass – equal to that of the continuous carbon baseline configuration – and a high, wide, flat plateau in the stress–strain response with 1.61% pseudo-ductile strain.
- The modulus and the plateau stress of each hybrid configuration were predicted accurately, successfully accounting for the effects of the platelet length and the platelet thickness. Therefore good overall agreement was obtained between the modelled and the measured stress–strain responses.

Acknowledgements

This work was funded under the UK Engineering and Physical Sciences Research Council Programme Grant EP/I02946X/1 on High Performance Ductile Composite Technology in collaboration with Imperial College London. The authors acknowledge Hexcel Corporation for supplying the S-glass/epoxy prepreg for this research.

References

[1] Hancox NL. Fibre composite hybrid materials. London: Applied Science Publishers Ltd.; 1981.
[2] Summerscales J, Short D. Carbon fibre and glass fibre hybrid reinforced plastics. Composites 1978;9:157–66.
[3] Short D, Summerscales J. Hybrids – a review Part 1. Techniques design and construction. Composites 1979;10:215–21.
[4] Short D, Summerscales J. Hybrids – a review Part 2. Physical properties. Composites 1980;11:33–8.
[5] Kretsis G. A review of the tensile, compressive, flexural and shear properties of hybrid fibre-reinforced plastics. Composites 1987;18:13–23.
[6] Marom G, Fischer S, Tuler FR, Wagner HD. Hybrid effects in composites: conditions for positive or negative effects versus rule-of-mixtures behaviour. J Mater Sci 1978;13(7):1419–26.
[7] Svensson N. Manufacturing of thermoplastic composites from commingled yarns – a review. J Thermoplast Compos Mater 1998;11(1):22–56.
[8] Diao H, Bismarck A, Robinson P, Wisnom MR. Pseudo-ductile behaviour of unidirectional fibre reinforced polyamide-12 composite by intra-tow hybridization. In: Proceedings of ECCM 15 Conference. Venice, June; 2012.
[9] Hayashi T. Development of new material properties by hybrid composition. 1st report. Fukugo Zairyo. Compos Mater 1972;1:18–20.
[10] Hayashi T, Koyama K, Yamazaki A, Kihira M. Development of new material properties by hybrid composition. 2nd report. Fukugo Zairyo. Compos Mater 1972;1:21–5.
[11] Bunsell AR, Harris B. Hybrid carbon and glass fibre composites. Composites 1974;5:157–64.
[12] Manders PW, Bader MG. The strength of hybrid glass/carbon fibre composites. J Mater Sci 1981;16:2233–45.
[13] Czél G, Wisnom MR. Demonstration of pseudo-ductility in high performance glass–epoxy composites by hybridisation with thin-ply carbon prepreg. Composites Part A 2013;52:23–30.
[14] Jalalvand M, Czél G, Wisnom MR. Numerical modelling of the damage modes in UD thin carbon/glass hybrid laminates. Compos Sci Technol 2014;94:39–47.
[15] Jalalvand M, Czél G, Wisnom MR. Damage analysis of pseudo-ductile thin-ply UD hybrid composites – a new analytical method. Composites Part A 2015;69:83–93.
[16] Sihn S, Kim RY, Kawabe K, Tsai SW. Experimental studies of thin-ply laminated composites. Compos Sci Technol 2007;67:996–1008.
[17] Yokozeki T, Aoki Y, Ogasawara T. Experimental characterization of strength and damage resistance properties of thin-ply carbon fiber/toughened epoxy laminates. Compos Struct 2008;82:382–9.
[18] Saito H, Morita M, Kawabe K, Kanesaki M, Takeuchi H, Tanaka M, et al. Effect of ply-thickness on impact damage morphology in CFRP laminates. J Reinf Plast Compos 2011;30:1097–106.
[19] Yokozeki T, Kuroda A, Yoshimura A, Ogasawara T, Aoki T. Damage characterization in thin-ply composite laminates under out-of-plane transverse loadings. Compos Struct 2010;93:49–57.
[20] Cui W, Wisnom MR, Jones MI. An experimental and analytical study of delamination of unidirectional specimens with cut central plies. J Reinf Plast Compos 1994;13:722–39.
[21] Wisnom MR, Jones MI. Delamination of unidirectional glass fibre–epoxy with cut plies loaded in four point bending. J Reinf Plast Compos 1995;14:45–59.
[22] Czél G, Pimenta S, Wisnom MR, Robinson P. Demonstration of pseudo-ductility in unidirectional discontinuous carbon fibre/epoxy prepreg composites. Compos Sci Technol 2015;106:110–9.
[23] Matthams TJ, Clyne TW. Mechanical properties of long-fibre thermoplastic composites with laser drilled microperforations 1. Effect of perforations in consolidated material. Compos Sci Technol 1999;59:1169–80.
[24] Matthams TJ, Clyne TW. Mechanical properties of long-fibre thermoplastic composites with laser drilled microperforations 2. Effect of prior plastic strain. Compos Sci Technol 1999;59:1181–7.
[25] Taketa I, Okabe J, Kitano A. A new compression- molding approach using unidirectionally arrayed chopped strands. Composites Part A 2008;39:1884–90.
[26] Li Hang, Wang Wen-Xue, Takao Yoshihiro, Matsubara Terutake. New designs of unidirectionally arrayed chopped strands by introducing discontinuous angled slits into prepreg. Composites Part A 2013;45:127–33.
[27] Fuller J, Wisnom MR. Damage suppression in thin ply angle-ply carbon/epoxy laminates. In: Proceedings of ICCM-19 conference. Montreal, July 2013; 2013.
[28] Wisnom MR, Atkinson JW. Reduction in tensile and flexural strength of unidirectional glass fibre–epoxy with increasing specimen size. Compos Struct 1997;38:405–11.
[29] Wisnom MR, Jones MI. Size effects in interlaminar tensile and shear strength of unidirectional glass fibre–epoxy. J Reinf Plast Compos 1996;15:2–15.
[30] Czél G, Jalalvand M, Wisnom MR. Development of pseudo-ductile hybrid composites with discontinuous carbon- and continuous glass prepregs. In: Proceedings of ECCM-16 conference. Seville, June, 2014; 2014.